Int J Adv Manuf Technol (2010) 46:913–921
DOI 10.1007/s00170-009-2033-8

SPECIAL ISSUE - ORIGINAL ARTICLE

Adaptive identification of hysteresis and creep in piezoelectric stack actuators

J. Minase · T.-F. Lu · B. Cazzolato · S. Grainger

Received: 14 December 2007 / Accepted: 24 March 2009 / Published online: 10 May 2009

Abstract The adaptive identification of the non-linear hysteresis and creep effects in a piezoelectric actuator is proposed in this paper. Model uncertainties related to the hysteresis and creep effects, most prominently in the high frequency zone (to 100 Hz), large operating amplitude and/long operating time, can make a piezoelectric actuator-driven micro-positioning system unstable in the closed loop. Furthermore, these uncertainties may lead to inaccurate open-loop control and frequently cause harmonic distortion when a piezoelectric actuator is driven with a sinusoidal input voltage signal. In order to solve the above issues, it is important to determine an accurate non-linear dynamic model of a piezoelectric actuator. An unscented Kalman filter-based adaptive identification algorithm is presented, which accurately determines the non-linear dynamics of a piezoelectric stack type actuator such that the non-linear hysteresis and creep effects can be accurately predicted. Since hysteresis and creep are dominant in open loop, the actuator is driven in an open-loop mode in this investigation.

Keywords Piezoelectric stack actuator · Hysteresis · Creep · Unscented Kalman Filter · Model identification

1 Introduction

A piezoelectric actuator consists of a piezoelectric crystal that expands or contracts when a positive or negative, voltage or charge, signal is applied. The displacement of a piezoelectric actuator is due to the ferroelectric nature of the crystal. Although charge control exists [1], the displacement of a piezoelectric actuator is commonly controlled using a voltage input [2–6] due to the ease of implementation. The resolution of a voltage-driven piezoelectric actuator is thus dependent only on the amount of disturbance noise in the voltage input and the resolution of the sensor used to measure the resulting displacement of a piezoelectric actuator. There are many micro-positioning applications that utilise a piezoelectric actuator for actuation purpose due to the requirement for nanometre resolution in displacement, large force exertion, high stiffness, fast response time and efficient energy conversion [5, 6]. Some of the many micro-positioning applications that utilise a piezoelectric actuator are scanning tunnelling microscopy [7], active vibration control of mechanical components [8], diamond turning machines [9], machine tool control [5] and micromotion stages [6, 10]. Unfortunately, when a voltage signal is applied to a piezoelectric actuator in open-loop mode, a non-linear displacement response with hysteresis and creep can be observed.

The remainder of this paper is organised as follows: The hysteresis and creep non-linearities are presented in the background study in Section 2. In Section 3, the adaptive identification of the non-linear hysteresis and creep effects in a piezoelectric actuator are presented. The experimental setup is presented in Section 4, and the results obtained from this investigation are presented in Section 5. Finally, the concluding remarks follow in Section 6.

2 Background

Hysteresis and creep can severely affect the precise positioning of a piezoelectric actuator driven micro-

J. Minase (✉) · T.-F. Lu · B. Cazzolato · S. Grainger
School of Mechanical Engineering, The University of Adelaide, Adelaide, SA 5005, Australia
e-mail: jayesh.minase@mecheng.adelaide.edu.au

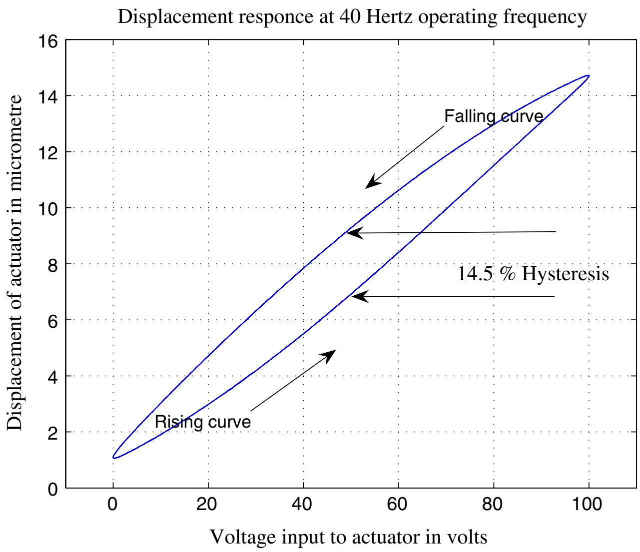

Fig. 1 Hysteresis in piezoelectric stack type actuator at 40 Hz operating frequency

positioning application. Using an inaccurate model of the non-linear dynamics of a piezoelectric actuator, which would lead to inaccurate prediction of hysteresis and creep, may lead to inaccurate control of a micro-positioning application [3, 5]. It is therefore important to determine accurately the non-linear dynamics (hysteresis and creep) of a piezoelectric actuator such that fast and accurate reference tracking of a micro-positioning application is possible.

Hysteresis, caused by the polarisation of microscopic ferroelectric particles [11], is said to be a rate-independent non-linearity [12, 13], which depends on a combination of the currently applied voltage as well as on past values of the applied voltage (memory). Although hysteresis does not depend on the past rate of the applied voltage signal, it changes with the amplitude of the applied voltage signal [14]. In addition, the non-linear hysteretic characteristic of a piezoelectric actuator can be non-differentiable at times [15]. When the voltage-driven piezoelectric actuator is operated in an open-loop mode, the maximum positioning error caused by the effect of hysteresis can be as much as 10–15% of the operative range of the actuator [13]. The effect of hysteresis, more pronounced over long range operations, can be minimised by operating the actuator in a linear range. This can be achieved by keeping the amplitude of the applied voltage signal constant and as small as possible. However, in such a case, the actuator's ability to be displaced over a long range with high precision needs to be sacrificed.

When a voltage signal is applied to a piezoelectric actuator, a non-linear displacement response with a hysteresis curve can be observed. In Fig. 1, the amount of hysteresis in a low voltage piezo (LVPZ) power amplifier-driven piezoelectric stack type actuator is determined by plotting the displacement of the actuator with respect to the voltage input to the actuator. The percentage hysteresis, for a specific input voltage value, is calculated as the ratio of the vertical length of the curve to the horizontal length of the curve. The vertical length is the difference between the rising and the falling displacement, both of which occur at the same value of input voltage, while the horizontal length is the difference between the displacement of the actuator at zero voltage and maximum voltage (100 V in this case). In Fig. 1, the maximum percentage hysteresis is 14.5% at 50% voltage swing, i.e., 50 V input to the actuator.

Creep, a slow eccentric drift in the displacement of a piezoelectric actuator [16, 17], is the effect of the applied high voltage signal on the remanent polarisation of a piezoelectric actuator. The creep behaviour, theoretically illustrated in Fig. 2, is more prominent over extended periods of time or in low bandwidth applications. In Fig. 2, the change in the amount of creep in the negative direction is due to the continuous decrease in the remanent polarisation of a piezoelectric actuator. This change is measured 0.1 s after the applied high voltage signal reaches a constant value. Creep affects the absolute positioning of a piezoelectric actuator in slow or static applications [18].

Fig. 2 Theoretical representation of the creep behaviour in a piezoelectric actuator in open loop

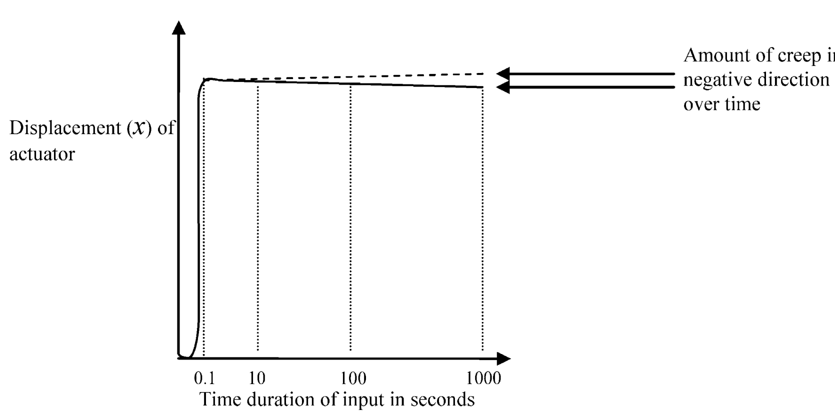

Operating a piezoelectric actuator fast enough can help reduce the positioning error caused by creep.

The combined effect of the non-linear hysteresis and creep is usually unknown, and the states that are required to represent its dynamics are not easily measured. The combined effect can lead to 15–20% inaccuracy in open-loop control (for operating frequency above 30 Hz) [13] and instability in closed loop control [2] of micro-positioning applications, which could reduce the effectiveness of feedback control [12]. It has been proven that the combined effect of hysteresis and creep can amount to about 50% error during calibration of a micro-positioning application [19]. Fast (operating frequency of around 100 Hz) and accurate reference tracking of a micro-positioning application therefore requires accurate determination of the dynamic model of a piezoelectric actuator such that the non-linear hysteresis and creep effects can be accurately predicted.

3 Adaptive identification

The dynamic modelling of a piezoelectric actuator including its non-linear hysteresis and creep is not straight forward. Numerous phenomenological [13, 20, 21] as well as analytical [4] models have been derived to predict rate-independent hysteresis in piezoelectric actuators. The accuracy of the above static models often reduces when the piezoelectric actuator is operated under uncertain conditions with different sets of inputs. However, none of the above models that predict hysteresis can predict the creep effect. Mostly, a logarithmic model has been used to predict the creep behaviour [17]. More recently, model identification based approaches have been found effective in precise estimation of the non-linear dynamics of piezoelectric actuators [2, 14, 22].The model identification approach integrates a nominal dynamic model of a piezoelectric actuator with its displacement measurements to predict the non-linear hysteresis behaviour. However, this approach is yet to be implemented in identification of creep.

State estimation, a model identification based approach, is the process of determining the unknown current states of a complex system, given the measurement observations recorded using a sensor and a nominal dynamic model. In doing so, the estimation algorithm needs to account for artefacts due to sensor inaccuracies, additive noise/distortions, nominal dynamic model imperfections and any unaccounted uncertainties. The Kalman Filter algorithm [23] is one of the most widely used methods in state estimation due to its simplicity, optimality in estimation of unknown current states and robustness. It is a set of mathematical equations that, in its discrete form, implement a predictor–corrector type approach to estimate the unknown current states of a complex system. Since the Kalman Filter algorithm estimates the states of a dynamic model that is assumed to be a set of linear stochastic differential equations, its application to non-linear dynamic systems can be difficult [24]. The unscented Kalman filter (UKF) algorithm proposed by Julier and Uhlmann [24] and further developed by Wan and Merwe [25] provides superior performance in state estimation for non-linear dynamic systems.

The UKF provides a deterministic sampling approach to capture the mean and covariance of a Gaussian, independent, white in nature, distribution of random variables. The UKF uses the unscented transformation method [26] to choose a minimal number of sample points such that the true mean and covariance of the random variables is completely captured. On propagation through the true dynamic model of a non-linear system, these sample points capture the posterior mean and covariance accurately to the third order[1] for Gaussian inputs. The structure of the UKF algorithm is presented in detail in Appendix A.

An UKF [25] based adaptive identification approach[2] is developed to accurately estimate the non-linear dynamics of a piezoelectric actuator such that the non-linear hysteresis and creep effects can be accurately predicted. The algorithm integrates a nominal dynamic model of a piezoelectric actuator with its displacement measurement updates in order to accurately estimate the non-linear dynamic model of a piezoelectric actuator. The estimated adaptive non-linear dynamics of the actuator helps predict the effect of hysteresis and creep precisely. The identification approach is presented in the form of a flow diagram in Fig. 3.

For adaptive identification of hysteresis using the UKF, the nominal dynamics of a piezoelectric actuator is presented in terms of a second-order linear parametric model coupled with a first-order non-linear hysteresis model [3]. The behaviour of a piezoelectric actuator that is assumed to have a lumped mass, a linear material stiffness and damping is given by

$$m_p\ddot{x} + b_p\dot{x} + k_p x = k_p(cv - h) \tag{1}$$

where x is the displacement of a piezoelectric actuator, m_p, b_p, k_p and c are the mass, damping, stiffness and piezoelectric coefficient of a piezoelectric actuator, h is the output variable of the dynamic model of non-linear

[1] Order refers to Taylor's series transformation.

[2] The UKF based adaptive identification approach is run in open-loop mode.

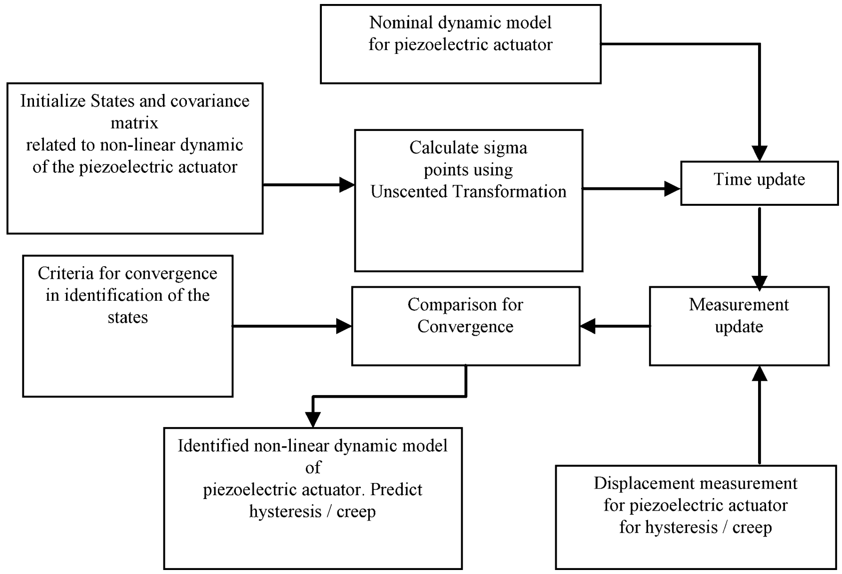

Fig. 3 Flow diagram for unscented Kalman filter based adaptive identification algorithm

hysteresis behaviour and v is the applied voltage signal. The first-order non-linear hysteresis model [3] is given by

$$\dot{h} = \mu c\dot{v} - \tau\left|\dot{v}\right|h - \delta v|h| \tag{2}$$

where μ, τ and δ are the constants that affect the shape of the hysteresis curve for a piezoelectric actuator. The linear parametric model in Eq. 1 and the first-order non-linear hysteresis model in Eq. 2 combine together to form the nominal state-space dynamic model of a piezoelectric actuator that describes the non-linear hysteresis effect. The coupled equations (Eqs. 1 and 2) can then be represented in a state-space matrix form by

$$\begin{aligned} \dot{X}(t) &= A(X) + Bu(t) \\ y(t) &= CX(t) \end{aligned} \tag{3}$$

where

$$\begin{aligned} &\mathrm{X}(t) = \left(x, \dot{x}, h, v, \dot{v}\right)^{\mathrm{T}} \\ &\mathrm{A(X)} = \begin{bmatrix} \dot{x} \\ -\left[k_p x + b_p\dot{x} - k_p h - k_p cv\right]\Big/ m_p \\ \mu c\dot{v} - \tau\left|\dot{v}\right|h - \delta\dot{v}|h| \\ \dot{v} \\ 0 \end{bmatrix} \\ &\mathrm{B} = \begin{bmatrix} 0 \\ 0 \\ 0 \\ 0 \\ 1 \end{bmatrix}, \mathrm{C}^{\mathrm{T}} = \begin{bmatrix} 1 \\ 0 \\ 0 \\ 0 \\ 0 \end{bmatrix} \end{aligned} \tag{4}$$

In Eq. 3, u (t) is the control input, and y (t) is the displacement measurement obtained from the actuator. In Eq. 4, $\underline{x}$ and $\underline{v}$ are the rate of change of displacement and the rate of change of voltage input, respectively.

For the adaptive identification of creep using the UKF, the nominal dynamics of a piezoelectric actuator is given by the second-order linear parametric model in Eq. 1. The hysteresis parameter h is taken to be zero in this case. The nominal dynamics can then be written as

$$m_p\ddot{x} + b_p\dot{x} + k_p x = k_p(cv) \tag{5}$$

4 Experimental setup

The block diagram of the experimental setup to measure the displacement of the piezoelectric actuator is shown in Fig. 4. The piezoelectric actuator used in the experiment is the Tokin model number AE0505D16 piezoelectric stack-type actuator (Fig. 5), which from here onwards is called the piezo actuator.

The maximum displacement of the piezo actuator is 17 mm, and the recommended operating voltage is 100 V. The piezo actuator was driven using a P-865.10 LVPZ power amplifier module with a voltage output range from −20 to +120 V and output power of 30 W. A fibre optic displacement sensor (Fig. 5) with 5 nm resolution was used to measure the displacement of the piezo actuator. A dSPACE ds1104 platform compatible with Matlab and Simulink software was used to interface the experimental setup to the computer, and a Simulink model was developed to drive the piezo actuator with a voltage input signal. To measure the amount of hysteresis

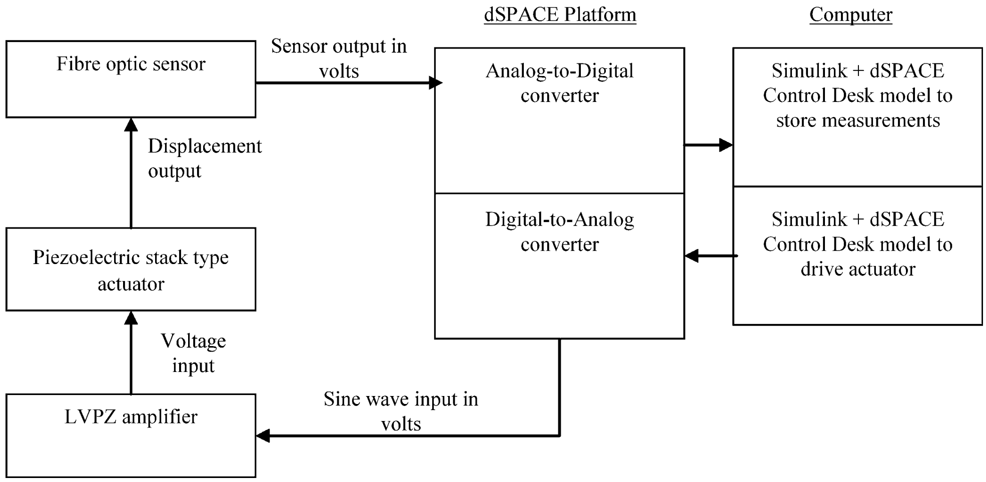

Fig. 4 Block diagram of experimental setup

in the piezo actuator in open loop, the piezo actuator was driven using a sinusoidal input voltage signal with voltage ranging from 0 to 100 V and operating frequency of up to 100 Hz. The amount of creep in the piezo actuator in open loop was measured by driving the piezo actuator using a step input voltage signal. A Matlab script was developed to execute the UKF-based adaptive identification algorithm. The values for different parameters of the nominal model (Eqs. 1, 2, 3, 4 and 5) are given in Table 1. The values for mass, stiffness and damping of the actuator were obtained from the specification sheet, while the values for the constants[3] μ, τ and δ that affect the shape of the hysteresis curve were determined offline from the hysteresis curve simulated using Eq. 2.

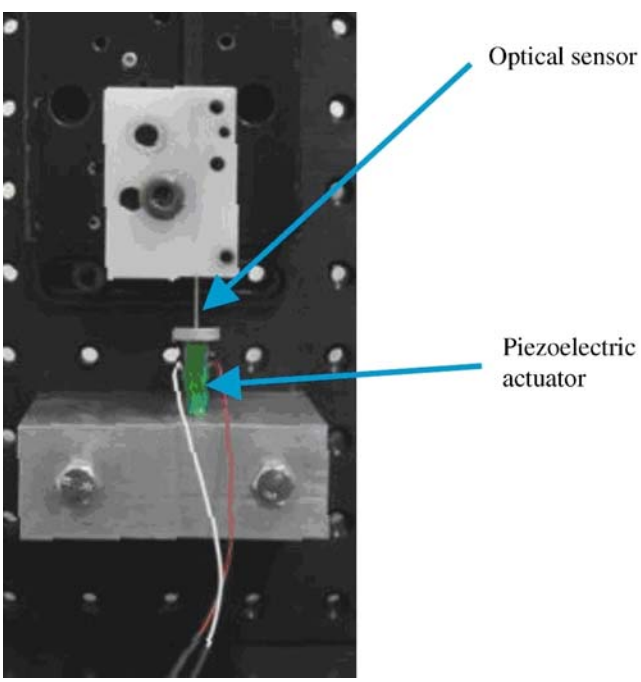

Fig. 5 Photograph of the piezoelectric stack-type actuator connected to the fibre optic sensor

5 Results

The percentage hysteresis in the piezo actuator was determined for an operating frequency of up to 100 Hz; the operating voltage signal was a 0 to 100 V sine wave. In Fig. 6, the maximum percentage hysteresis in the piezo actuator is plotted against operating frequency between 0 to 100 Hz. The amount of hysteresis in the piezo actuator is seen to increase with the operating frequency. This shows that, although hysteresis in the piezo actuator is approximately rate independent at lower operating frequencies, at higher operating frequencies, it is in fact dependent on the rate (frequency) at which the input voltage is applied. Thus, static models discussed in Section 3 will be unable to predict such rate-dependent hysteresis. The UKF-based approach, which is adaptive to changes in behaviour of a non-linear system, would thus be useful in predicting such hysteresis.

In Fig. 7, it can be seen that the maximum amount of hysteresis in the piezo actuator is 23%. The error in identification of the hysteresis, presented (Fig. 8) for the case where the piezo actuator is driven at an operating frequency of 100 Hz and an amplitude of 0 to 100 V, is determined by subtracting the identified hysteresis from the experimentally measured hysteresis. As shown in Fig. 8, the maximum percentage error in the identification of

[3] The value for the constants changes with the shape of the hysteresis curve. Range identified for the complete set of experiments in presented.

Table 1 Values of parameters of the nominal model

Parameter	Value
m_p	0.004 kg
b_p	150 N-s/m
k_p	6×10^6 N/m
c	635×10^{-12} m/V
μ	0.5–0.7
τ	0.01–0.03
δ	−0.15

hysteresis is approximately 3.2 % of the maximum displacement of the piezo actuator. As the identification algorithm was run in real time and the measurement updates taken after every tenth time step, by the UKF algorithm, it can be concluded that the UKF-based identification process is adaptive and performs accurately over a prolonged period of time.

As shown in Fig. 6, hysteresis in the piezo actuator increases with the operating frequency. The adaptability of the UKF-based identification algorithm to such change was tested by running the identification process for different operating frequencies. In Fig. 9, the maximum percentage error in identification of hysteresis using the UKF-based adaptive identification algorithm is plotted against operating frequency from 0 to 100 Hz. It can be seen that the adaptive identification algorithm accurately estimates hysteresis over a wide range of operating frequency. Although there is an approximately linear increase in the amount of percentage hysteresis (Fig. 6), the maximum percentage error in identification of the hysteresis effect is approximately 3% for operating frequencies between 30 and 100 Hz. It can thus be inferred that the adaptive identification approach is stable enough in the identification of hysteresis in the actuator over wide range of operating frequencies. When compared to other approaches, like the multi-polynomial approach [27], which reduces the error in the identification of hysteresis to below 1% for similar range of operating frequencies, the percentage error in the identification of hysteresis using the UKF-based algorithm seems to be on the higher side at higher operating frequencies. This error could further be reduced by taking measurement updates at every time step (instead of every tenth time step as mentioned previously). However, with the increase in the number of measurement samples, the processing time taken by the identification algorithm, to accurately predict hysteresis, will increase as well. Thus,

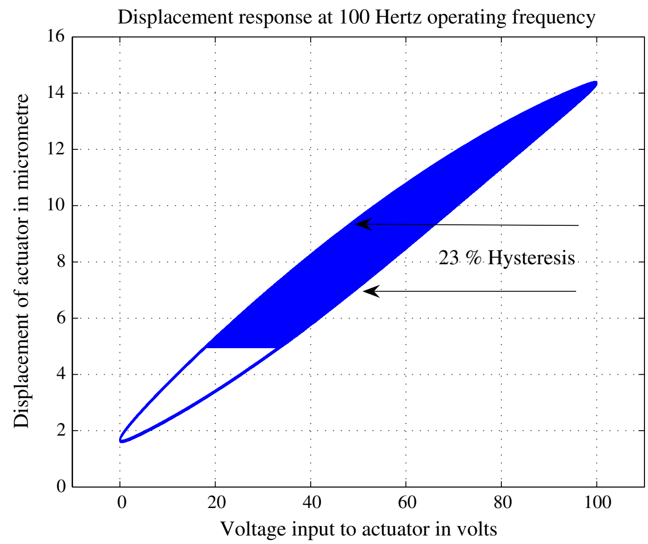

Fig. 7 Hysteresis in piezo actuator at 100 Hz operating frequency

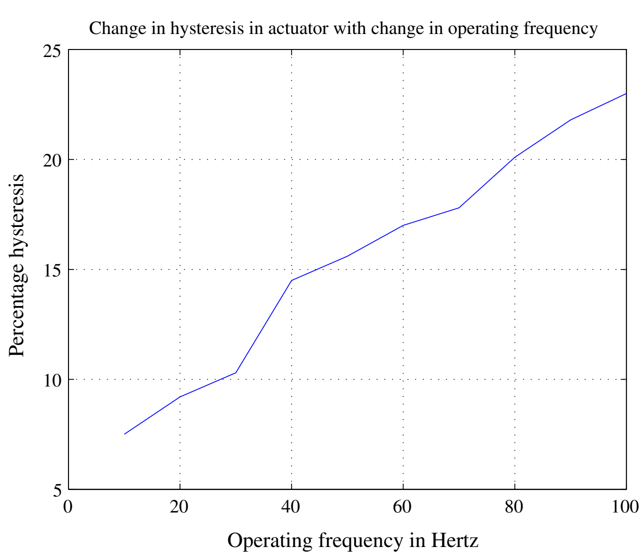

Fig. 6 Effect of operating frequency on hysteresis in the piezo actuator

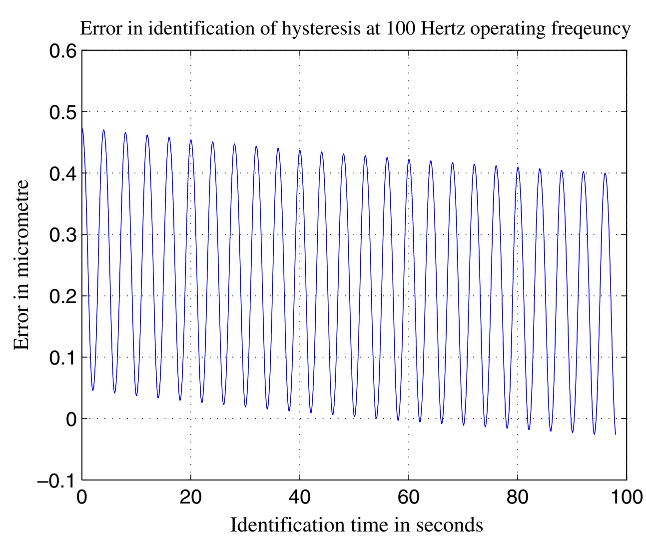

Fig. 8 Error in identification of hysteresis in piezo actuator at 100 Hz

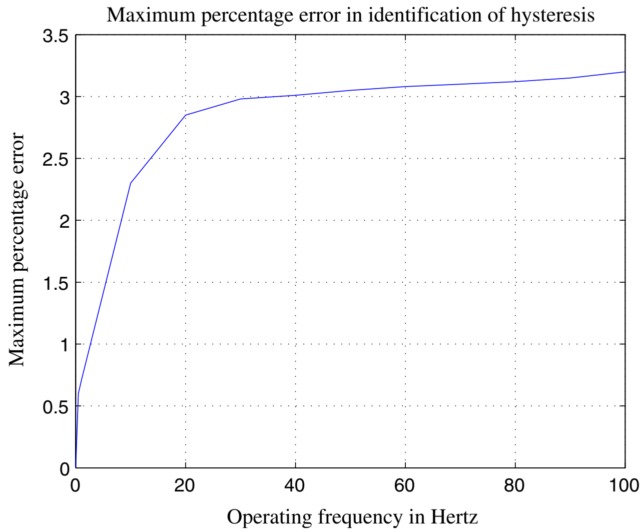

Fig. 9 Maximum percentage error in identification of hysteresis in piezo actuator at different operating frequencies

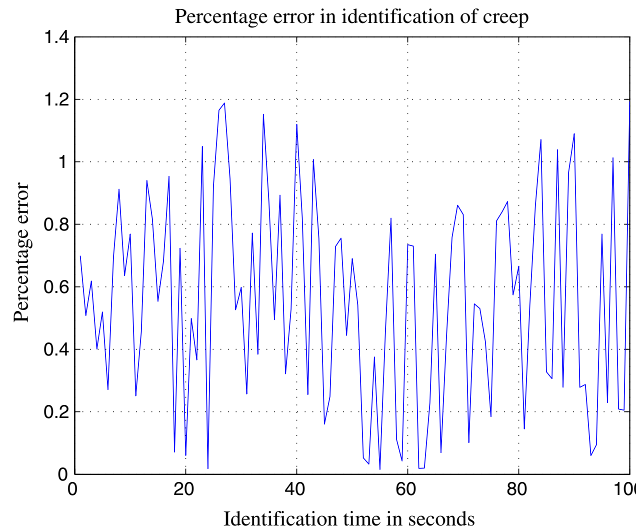

Fig. 11 Percentage error in identification of creep for a 100-V step input

there exists a tradeoff between the minimum error that can be achieved and the processing time taken by the algorithm. However, it is worth mentioning that the use of a faster digital signal processor board or a parallel processing field-programmable gate array could well reduce the processing time taken by the algorithm.

The result for identification of the creep effect is presented for the case where the piezo actuator is driven using a step input of 100 V. The measured creep effect is presented in Fig. 10. The creep effect, over the duration of the step input, was measured with respect to location L_0, 0.1 s after the step input reached a constant value of 100 V. The maximum creep, around 8.9%, is observed at time equal to 60 s. The percentage error in identification of the creep effect using the UKF-based adaptive identification algorithm is depicted in Fig. 11. The percentage error was determined by subtracting the identified creep from the experimentally measured creep. The maximum percentage error is 1.2% of the maximum displacement of the piezo actuator. In Fig. 12, the maximum percentage error in identification of creep using the UKF-based adaptive identification algorithm is plotted against step input commands between 0 and 100 V. Although the error in identification of creep increases with the step input, it still remains in reasonable bounds. Further reduction in error might be achieved by using the logarithmic model [17] as a nominal dynamic model in the creep identification process.

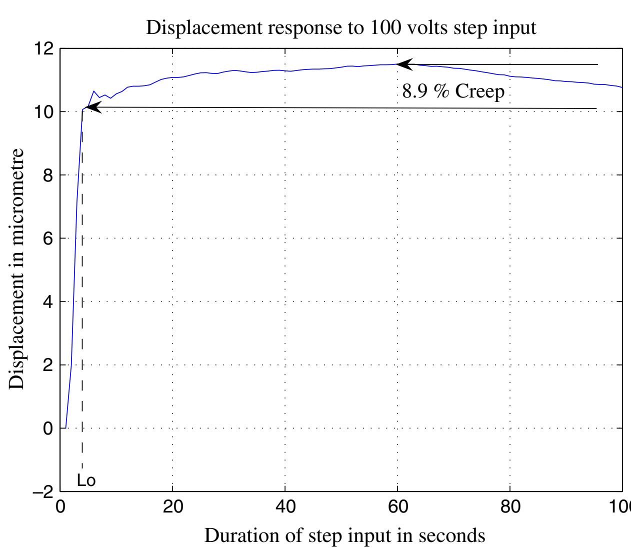

Fig. 10 Measured creep effect in piezo actuator for a 100-V step input applied for duration of 100 s

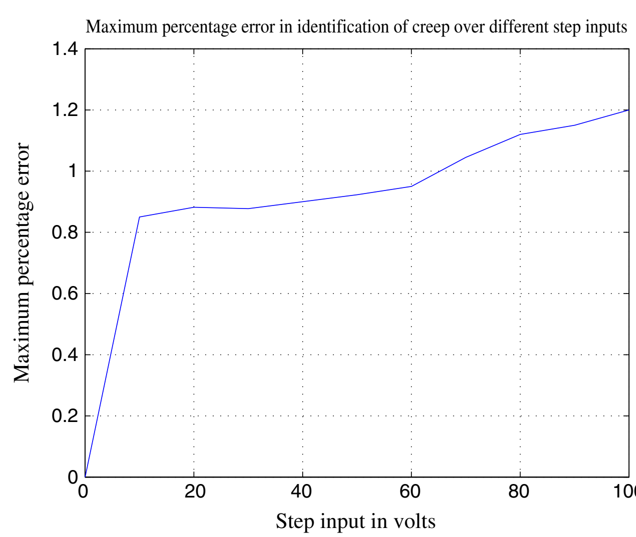

Fig. 12 Maximum percentage error in identification of creep over different step inputs

6 Conclusion

The proposed UKF-based adaptive identification approach accurately determines the non-linear dynamics of the piezo actuator. The identified dynamics accurately predicts the non-linear hysteresis and creep effects in the piezo actuator. The accurately identified model of the piezo actuator will thus be helpful in fast and accurate control of micro-positioning applications. Future work will focus on implementation of the UKF-based adaptive identification approach in the identification of non-linear dynamics of other type of piezoelectric actuators, which exhibit similar hysteresis and creep effects.

Appendix A

Unscented Kalmen filter algorithm

Initialise with

$$\widehat{X}_0 = E[X_0]$$

$$P_0 = E\left[\left(X_0 - \widehat{X}_0\right)\left(X_0 - \widehat{X}_0\right)^T\right]$$

$$\widehat{X}_0^a = E[X^a] = \left[\widehat{X}_0^T 00\right]^T$$

$$P_0^a = \begin{bmatrix} P_0 & 0 & 0 \\ 0 & R^V & 0 \\ 0 & 0 & R^n \end{bmatrix}$$

For k∈{1,…….,∞} Calculate sigma points

$$\chi_{k-1}^a = \left[\widehat{X}_{k-1}^a, \widehat{X}_{k-1}^a + \gamma\sqrt{P_{k-1}^a}, \widehat{X}_{k-1}^a - \gamma\sqrt{P_{k-1}^a}\right]$$

Time update equation

$$\chi_k^X = F\left[\chi_{k-1}^X, u_{k-1}, \chi_{k-1}^V\right] \quad , \quad \widehat{X}_k^- = \sum_{i=0}^{2L} W_i^{(m)} \chi_{i\ ,\ k|k-1}^X$$

$$P_k^- = \sum_{i=0}^{2L} W_i^{(c)} \left[\chi_{i\ ,\ k|k-1}^X - \widehat{X}_k^-\right]\left[\chi_{i\ ,\ k|k-1}^X - \widehat{X}_k^-\right]^T$$

$$y_{k|k-1} = H\left[\chi_{k|k-1}^X, X_{k-1}^n\right] \quad , \quad \widehat{y}_k^- = \sum_{i=0}^{2L} W_i^{(m)} y_{i\ ,\ k|k-1}$$

Measurement update equation

$$P_{\widetilde{y}_k\widetilde{y}_k} = \sum_{i=0}^{2L} W_i^{(c)} \left[y_{i,\ k|k-1} - \widehat{y}_k^-\right]\left[y_{i,\ k|k-1} - \widehat{y}_k^-\right]^T$$

$$P_{X_k y_k} = \sum_{i=0}^{2L} W_i^{(c)} \left[\chi_{i,\ k|k-1} - \widehat{X}_k^-\right]\left[y_{i,\ k|k-1} - \widehat{y}_k^-\right]^T$$

$$K_k = P_{X_k y_k} P_{\widetilde{y}_k\widetilde{y}_k}^{-1}$$

$$\widehat{X}_k = \widehat{X}_k^- + K_k\left(y_y - \widehat{y}_k^-\right)$$

$$P_k = P_k^- - K_k P_{\widetilde{y}_k\widetilde{y}_k} K_k^T$$

where

$$X^a = \left[X^T, V^T, n^T\right]^T \tag{6}$$

Appendix B

List of symbols

x	Displacement of the piezoelectric stack type actuator
m_p	Mass of the piezoelectric stack type actuator
b_p	Damping of the piezoelectric stack type actuator
k_p	Stiffness of the piezoelectric stack type actuator
c	Piezoelectric coefficient of the piezoelectric stack type actuator
h	The output variable of the dynamic model of non-linear hysteresis behaviour
v	Applied voltage signal
μ, τ, and δ	Constants that affect the shape of the hysteresis curve
u (t)	Control input
y (t)	Displacement measurement obtained from the piezoelectric stack type actuator
$\dot{x}$	Rate of change of displacement of the piezoelectric stack type actuator
$\dot{v}$	Rate of change of voltage input the piezoelectric stack type actuator
$\widehat{X}_0$	Original state vector
X_0^a	Augmented state vector formed by concatenation of state vector by adding measurement and covariance noise variables
V	Process noise
n	Measurement noise
P_0	Covariance for original state vector
P_0^a	Covariance for augmented state vector
R^v	Process noise covariance
R^n	Measurement noise covariance
k	Time step for simulation
γ	(L + λ)
L	Length of augmented state vector
λ	Scaling variable
χ_k^a	Sigma points for augmented state vector
W_i	Weights calculated using Equation (2.23)
$\widehat{X}_k^-$	A priori estimate of augmented state vector
P_k^-	A priori error covariance
$\widehat{y}_k^-$	A priori estimate of measurement
$P_{\widetilde{y}_k\widetilde{y}_k}$	A priori measurement error covariance
$P_{X_k y_k}$	A priori cross covariance between apriori state and measurement estimate
K_k	Gain
y_k	True measurement
$\widehat{y}_k$	Estimated measurement

$\widehat{X}_k$ A posteriori state estimate
P_k Aposteriori error covariance

Appendix C

Other formulas used

$$1.\text{Error} = \text{Identified value} - \text{Measured value}$$

$$2.\text{Percentage error} = \frac{\text{Identified value} - \text{Measured value}}{\text{Measured value}}$$

$$3.\text{Percentage creep} = \frac{\text{Maximum displacement of actuator} - \text{Displacement of actuator at } L_0}{\text{Maximum displacement of actuator}}$$

$$4.\text{Percentage hysteresis} = \frac{\text{Rising curve displacement} - \text{Falling curve displacement}}{\text{Displacement (max input voltage)} - \text{displacement (min input voltage)}}$$

References

1. Newcomb CV, Flinn I (1982) Improving the linearity of piezoelectric ceramic actuators. IEEE Electron Lett 18(11):442–442. doi:10.1049/el:19820301
2. Huang S, Tan K, Lee T (2002) Adaptive motion control using neural network approximations. Automatica 38(2):227–233. doi:10.1016/S0005-1098(01)00192-3
3. Jan C, Hwang C (2000) Robust control design for a piezoelectric actuator system with dominant hysteresis. IEEE Int Conf Ind Electron Instrum 3:1515–1520
4. Goldfarb M, Celanovic N (1997) A lumped parameter electromechanical model for describing the nonlinear behaviour of piezoelectric actuators. J Dyn Syst Meas Control 119:478–485. doi:10.1115/1.2801282
5. Mayhan P, Srinivasan K, Watechagit S, Washington G (2000) Dynamic modelling and controller design for a piezoelectric actuation system used for machine tool control. J Intell Mater Syst Struct 11(10):771–780
6. Handley D, Lu T-F, Yong YK, Eales C (2004) Workspace investigation of a 3DOF compliant micro-motion stage. The 8th International Conference on Control, Automation, Robotics and Vision, ICARCV
7. Stroscio J, Kaiser W (1993) Scanning tunneling microscopy. Academic, San Diego
8. Palazzolo A, Jagannathan S, Kascak A, Montague G, Kiraly L (1993) Hybrid active vibration control of rotor bearing systems using piezoelectric actuators. J Vib Acoust 115:111–119. doi:10.1115/1.2930303
9. Okazaki Y (1990) A micro positioning tool post using a piezoelectric actuator for diamond turning machines. Precis Eng 12(3):151–156. doi:10.1016/0141-6359(90)90087-F
10. Yong YK, Lu T-F, Minase JL (2006) Trajectory following with a three-DOF micro-motion stage. Australasian Conference on Robotics and Automation, ACRA, December 6–8, Auckland, New Zealand
11. Huang L, Tiersten H (1998) An analytical description of slow hysteresis in polarized ferroelectric ceramic actuators. J Intell Mater Syst Struct 9:417–426
12. Arafa M, Baz A (2004) On the nonlinear behaviour of piezoelectric actuator. J Vib Control 10(3):387–398. doi:10.1177/1077546304033365
13. Ge P, Jouaneh M (1995) Modelling hysteresis in piezoceramic actuators. Precis Eng 17(3):211–221. doi:10.1016/0141-6359(95)00002-U
14. Minase J, Lu T, Wornle F (2007) State estimation of non-linear piezoelectric stack actuator hysteresis model. Proc SPIE Int Soc Opt Eng 6414:1–10
15. Adriaens H, De Koning W, Banning R (2000) Modelling piezoelectric actuators. IEEE/ASME Trans Mechatron 5(4):331–341. doi:10.1109/3516.891044
16. Tokin (2000) Multilayer piezoelectric actuators (product guide), 1 (1)
17. Ru C, Sun L (2005) Hysteresis and creep compensation for piezoelectric actuator in open-loop operation. Sens Actuators A 122(1):124–130. doi:10.1016/j.sna.2005.03.056
18. Fett T, Thun G (1998) Determination of room-temperature tensile creep of PZT. J Mater Sci Lett 17:1929–1931. doi:10.1023/A:1006608509876
19. Barrett R, Quate C (1991) Optical scan-correction system applied to atomic force microscopy. Rev Sci Instrum 62(6):1393–1399. doi:10.1063/1.1142506
20. Mayergoyz I (1986) Mathematical models of hysteresis. Phys Rev Lett 56:1518–1521. doi:10.1103/PhysRevLett.56.1518
21. Krasnosekl'skii M, Pokrovskii A (1983) Systems with hysteresis. Nauka, Moscow
22. Tong Z, Sui S, Du C (2006) A novel neural network model of hysteresis nonlinearities. Proceedings of the 6th International Conference on Intelligent Systems Design and Applications, 84–89
23. Kalman R (1965) A new approach to linear filtering and prediction problems. J Basic Eng Ser D 82:35–45
24. Julier S, Uhlmann J (1997) A new extension of the Kalman filters to nonlinear systems. In Proceedings of Aerosense: The 11th International Symposium on Aerospace/Defence Sensing, Simulation and Controls, pp 182–193
25. Wan E, Merve R (2001) Chapter 7: Unscented Kalman filter. Kalman filtering and neural networks. Wiley, New York
26. Julier S, Uhlmann J (1996) A general method for approximating non-linear transformations of probability distributions. Technical Report, Robotics Research Group, Department of Engineering Science, University of Oxford
27. Tse S, Gao Y (2007) Modelling of piezoelectric actuator based nano positioning system using multi polynomial regression with CI continuity. Key Eng Mater 339:434–441. doi:10.4028/www.scientific.net/KEM.339.434